The purification and steady-state kinetic behaviour of rabbit heart mitochondrial NAD(P)$^+$ malic enzyme

Vincent J. DAVISSON* and Arthur R. SCHULZ†
Department of Biochemistry, Indiana University School of Medicine, Indianapolis, IN 46223, U.S.A.

The mitochondrial NAD(P)$^+$ malic enzyme [EC 1.1.1.39, L-malate:NAD$^+$ oxido-reductase (decarboxylating)] was purified from rabbit heart to a specific activity of 7 units (μmol/min)/mg at 23°C. A study of the reductive carboxylation reaction indicates that this enzymic reaction is reversible. The rate of the reductive carboxylation reaction appears to be completely inhibited at an NADH concentration of 0.92mM. A substrate saturation curve of this reaction with NADH as the varied substrate describes this inhibition. The apparent kinetic parameters for this reaction are K_a(NADH) = 239μM and V_r = 1.1μmol/min per mg at 23°C. The steady-state product-inhibition patterns for pyruvate and NADH indicate a sequential binding of the substrates: NAD$^+$ followed by L-malate. These data also indicate that NADH is the last product released. A steady-state kinetic model is proposed that incorporates NADH–enzyme dead-end complexes.

The mitochondrial NAD(P)$^+$ malic enzyme [EC 1.1.1.39, L-malate:NAD$^+$ oxidoreductase (decarboxylating)] was first described and purified from *Ascaris suum* and later described in cauliflower and a group D streptococcus (Fodge *et al.*, 1972; Macrae, 1971). The enzyme has been partially purified from rabbit heart (Lin & Davis, 1974), from calf adrenal cortex (Mandella & Sauer, 1975; Sauer, 1973), from ascites L-1210 tumour cells (Hansford & Lehninger, 1973) and from dog small-intestinal mucosa (Nagel & Sauer, 1982). Thorough kinetic studies have been reported with the enzyme from *Ascaris suum* (Landsperger *et al.*, 1978), cauliflower (Canellas & Wedding, 1980; Canellas *et al.*, 1983; Grissom *et al.*, 1983) and potato (Grover *et al.*, 1981).

Previous reports concerning the properties of the NAD(P)$^+$ malic enzyme from mammalian cells indicate that the enzyme does not catalyse the reductive carboxylation of pyruvate (Lin & Davis, 1974; Mandella & Sauer, 1975). This is in contrast with the NADP$^+$ malic enzymes and other NAD(P)$^+$ malic enzymes (Hsu *et al.*, 1967; Frenkel, 1975; Landsperger *et al.*, 1978). A thermodynamic barrier for the reverse reaction is therefore not founded, and a reasonable conjecture

is that the apparent irreversibility is a kinetic phenomenon. The initial direction of the present work was to establish the basis for the kinetic irreversibility and to apply the findings to a more general mechanistic understanding of the enzyme.

Materials and methods

Materials

The following reagents were purchased from Sigma Chemical Co. (St. Louis, MO, U.S.A.): pyruvic acid, L-malic acid, oxaloacetic acid, oxamic acid, glutamic acid, dithiothreitol, bovine serum albumin and the protein M_r markers. The following reagents were purchased from Boehringer Mannheim Biochemicals (Indianapolis, IN, U.S.A.): NAD$^+$, NADP$^+$, NADH malate dehydrogenase (EC 1.1.1.37), lactate dehydrogenase (EC 1.1.1.27), glutamate–oxo-acid aminotransferase (EC 2.6.1.1) and triethanolamine hydrochloride. The following reagents were purchased from Fisher Scientific Co. (Fair Lawn, NJ, U.S.A.): MnCl$_2$, Na$_2$HPO$_4$, KH$_2$PO$_4$, Na$_2$CO$_3$, KHCO$_3$, disodium EDTA, NaN$_3$ and imidazole. The following reagents were purchased from BioRad Laboratories (Richmond, CA, U.S.A.): Coomassie Blue, acrylamide, bisacrylamide, ammonium persulphate, *NNN′N′*-tetramethyl-ethylenediamine and glycine. Enzyme-grade

* Present address: Department of Chemistry, University of Utah, Salt Lake City, UT 84102, U.S.A.
† To whom correspondence should be addressed.

$(NH_4)_2SO_4$ was purchased from ICN Nutritional Biochemicals (Cleveland, OH, U.S.A.). The ethylene glycol was purchased from the Aldrich Chemical Co. (Milwaukee, WI, U.S.A.). The phenyl-Sepharose was a product of Pharmacia Fine Chemicals (Piscataway, NJ, U.S.A.), and the DE52 DEAE-cellulose was a product of Whatman Chemical Separations (Clifton, NJ, U.S.A.). The sucrose, Tris and Hepes were products of Calbiochem (Los Angeles, CA, U.S.A.).

Enzyme assays

The oxidative decarboxylase assays of the mitochondrial malic enzymes were designed in accordance with published methods (Lin & Davis, 1974). The production of the appropriate nucleotide was continuously monitored as an increase in absorbance at 340 nm on a Cary 1605 spectrophotometer. The assays used to monitor the purification were performed at 23°C, and the kinetic studies were performed at 32°C. The standard reaction mixture of the NAD(P)$^+$ malic enzyme contained 300 μmol of triethanolamine/HCl buffer, pH 7.05, 3.0 μmol of $MnCl_2$, 45 μmol of L-malic acid, pH 6.9, and 1.5 μmol of NAD$^+$, pH 6.9, in a total volume of 1.5 ml. When the crude extracts were contaminated with lactate dehydrogenase, the assay mixture included 0.45 mM-oxamic acid, a competitive inhibitor of lactic acid (Webb, 1966). In cases where malate dehydrogenase was present, 5 units (μmol/min) of commercial malate dehydrogenase were included to ensure equilibrium of this enzymic reaction.

The pyruvate product-inhibition studies of the NAD(P)$^+$ malic enzyme utilized an Aminco SPF 125 spectrofluorimeter interfaced with a Processor Technology Sol-20 microprocessor for data acquisition and analysis. The excitation wavelength was 350 nm and the fluorescence emission wavelength was 450 nm (Lowry & Passonneau, 1972). The concentrations of reagents were similar to those described for the spectrophotometric assay.

Studies to quantify the production of NAD$^+$ and malate by the purified NAD(P)$^+$ malic enzyme were conducted at 23°C and were monitored at 366 nm in an Eppendorf model 1100 photometer equipped with a digital voltage display. The reaction mixtures contained 105 μmol of Hepes/NaOH buffer, pH 7.1, 15 μmol of pyruvic acid, pH 6.9, 37.5 μmol of KHCO$_3$, pH 7.8, 0.75 μmol of MnCl$_2$ and 0.056 μmol of NADH, pH 10.2, in a total volume of 0.75 ml at final pH 7.3. The reactions were stopped by the addition of 100 μl of 2M-HClO$_4$ and were kept at room temperature for 10 min before being cooled at 4°C and neutralized with K_2CO_3. The L-malic acid assay was a modification of a known enzymic assay and was standardized for this specific application (Moller-

ing, 1974). Studies of the kinetics of reductive carboxylase employed a Cary 1605 spectrophotometer at 340 nm. The reaction mixture contained 180 μmol of triethanolamine/HCl buffer, pH 7.0, 40 μmol of pyruvic acid, pH 7.2, 1.2 μmol of MnCl$_2$, 142 μmol of KHCO$_3$ pH 7.8, 0.0115–0.92 μmol of NADH, pH 10.2, and 7.5 μg of NAD(P)$^+$ malic enzyme in a total volume of 1.0 ml at final pH 7.4 at 23°C.

Phenyl-Sepharose chromatography

The 33–55%-satn.-$(NH_4)_2SO_4$-fraction pellet was resuspended immediately in a minimal volume of buffer. This buffer contained 25 mM-$(NH_2)SO_4$, 25 mM-KH_2PO_4, pH 6.9, 0.2 mM-EDTA and 0.50 mM-dithiothreitol (buffer A). After application of the suspension, the column was washed with 60 ml of buffer A and then washed with 200 ml of a buffer containing 15 mM-KH_2PO_4, pH 6.9, 0.2 mM-EDTA and 0.50 mM-dithiothreitol. The NAD(P)$^+$ malic enzyme was eluted with a linear gradient of decreasing ionic strength and increasing ethylene glycol concentration: 280 ml of solution containing 5 mM-KH_2PO_4, 0.2 mM-EDTA and 0.5 mM-dithiothreitol versus 220 ml of solution containing 5 mM-imidazole, 0.5 mM-dithiothreitol and 70% (v/v) ethylene glycol. The pooled fractions were dialysed against 2 litres of a buffer containing 20 mM-Tris, pH 8.0, 0.2 mM-EDTA and 0.5 mM-dithiothreitol.

DEAE-cellulose ion-exchange chromatography

The concentrated protein suspension from the phenyl-Sepharose chromatography was applied to a 2.4 cm × 7.5 cm column of DE52 DEAE-cellulose. After the application, the column was washed with 250 ml of the same buffer made 80 mM with respect to KCl. The enzyme was eluted with an increasing ionic-strength gradient. Those fractions of highest specific activity were pooled and concentrated to 10 ml by ultrafiltration on an Amicon PM10 membrane.

The concentrated protein suspension from the anion-exchange chromatography was vacuum-dialysed in a collodion bag against 150 ml of a buffer containing 20 mM-Tris, pH 7.8, 0.5 mM-EDTA and 1 mM-dithiothreitol at 4°C. The final protein concentration was approx. 0.3 mg/ml in a total volume of 2.0 ml.

Analysis of kinetic data

The estimates of initial velocities were obtained with specially written computer programs that utilized either the method of Walter & Barrett (1969) or a linear least-squares analysis. Estimates of the apparent Michaelis constants and maximum velocities were obtained by analyses of the initial-

velocity data (Wilkinson, 1961). A linear least-squares program with a proper statistical-error analysis was employed to obtain the inhibition constants. All values of the substrate and inhibitor concentrations were uncorrected for metal ion complexes.

The data for the substrate saturation curve of NADH in the reductive carboxylase reaction were fitted to an equation for complete substrate inhibition (Cleland, 1979).

The NADH product-inhibition data were fitted to a general second-order polynomial by least-squares regression analysis. Derivation of the rate equations for the kinetic models was accomplished with an implementation of the connection-matrix method (Fisher & Schulz, 1969).

Results and discussion

Enzyme purification

The NAD(P)+ malic enzyme has been purified from rabbit cardiac tissue to a specific activity of 7 units/mg at 23°C. This constitutes an 82-fold purification from the soluble mitochondrial extract and was achieved with 35% recovery. To date, this is the greatest degree of purification of this enzyme from this tissue. The data in Table 1 summarize the purification of the rabbit heart mitochondrial NAD(P)+ malic enzyme. The isolation, extraction and fractionation of the rabbit heart mitochondria were similar to methods described previously (Lin & Davis, 1974). A key step was the phenyl-Sepharose chromatography. The elution profile in Fig. 1 displays the utility of this step in removing the lactate dehydrogenase (extramitochondrial in origin) and 99% of the malate dehydrogenase. A linear gradient of ethylene glycol successfully eluted the desired enzyme in good yield with no apparent deleterious effects. The subsequent an-

ion-exchange chromatography successfully resolved the NAD(P)+ malic enzyme from the residual malate dehydrogenase. This resolution was most efficiently achieved when an isocratic step in ionic strength was employed. The sodium dodecyl sulphate/9.5%-polyacrylamide-gel electrophoresis of the final preparation indicated one major band of M_r 62200 and three minor bands.

Reductive carboxylation of pyruvate by NAD(P)+ malic enzyme

The most significant discovery of this work was the substrate inhibition by NADH in the reductive carboxylation reaction catalysed by the NAD(P)+ malic enzyme. Failure to recognize this phenomenon in earlier studies no doubt led other investigators to report the irreversibility of the reaction catalysed by this enzyme. To verify that
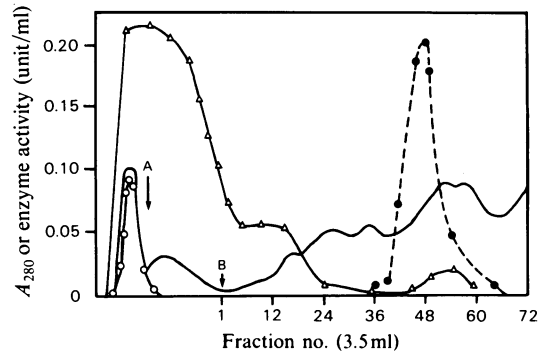

Fig. 1. *Phenyl-Sepharose chromatography of NAD(P)+ malic enzyme*
For full experimental details see the text. A, 0.015M-KH_2PO_4; B, start of linear gradient. ——, A_{280}; O, lactate dehydrogenase; △, malate dehydrogenase; ●, NAD[P]+ malic enzyme.

Table 1. *Purification of NAD(P)+ malic enzyme*
For full experimental details see the text. All values represent average values from 15 rabbit preparations. The assays of the crude extracts contained oxamic acid and commercial malate dehydrogenase (see the Materials and methods section). The assay of the 33–55%-satn.-$(NH_4)_2SO_4$ fraction was performed after resuspension of a small portion of the pellet in the extract buffer; the remainder of the pellet was resuspended in buffer A. The protein concentration of the DEAE-cellulose fraction was determined by relative absorbance at 280nm before the vacuum-dialysis.

Fraction	Volume (ml)	Protein (mg)	Total activity (units)	Sp. activity (units/mg)	Purification (fold)	Yield (%)
Mitochondrial sonicated extract	15.7	160	13.5	0.084	1	100
33–55%-satn.-$(NH_4)_2SO_4$ fraction	9.60	50	13.0	0.260	3	96
Phenyl-Sepharose fraction	45.0	10.8	10.8	1.00	12	80
DE52 DEAE-cellulose fraction	1.75	0.58	4.7	7.00	82	35

this enzymic oxidation was in fact the reverse reaction catalysed by the NAD(P)$^+$ malic enzyme, the NAD$^+$ and malate production were quantified in several incubations. The results of these experiments are provided in Table 2. These data indicate the proper stoichiometry for the reverse reaction and represent the first conclusive evidence for the reversibility of this enzyme.

To document more fully the apparent inhibition of the reductive carboxylation reaction by the substrate NADH, the initial velocity of NAD$^+$ production was measured at varied concentrations of NADH. Fig. 2 is a double-reciprocal graphical display of these data. There was no observable rate at an NADH concentration of 920 μM. Analysis of the data yielded estimates of 239 $\pm$ 16 μM for the apparent Michaelis constant for NADH and 1.1 μmol/min per mg for the apparent maximum velocity.

Apparent kinetic parameters for L-malate and NAD$^+$

There have been several previous reports that non-hyperbolic kinetics were observed when L-malate was the varied substrate (Mandella & Sauer, 1975; Sauer, 1973a, b). Table 3 displays the estimates of the apparent kinetic parameters for L-malate and NAD$^+$ under several assay conditions. There were no indications of non-hyperbolic initial-velocity patterns in any of these experiments, although approximately the same substrate concentration range was studied. These estimates of apparent Michaelis constants are in accord with those determined in previous investigations (Sauer, 1973a; Lin & Davis, 1974; Mandella & Sauer, 1975).

Product inhibition by NADH

In view of the complex effect of NADH concentration on the kinetics of the reductive carboxylation, a product-inhibition study of this

nucleotide in the forward reaction was performed. The double-reciprocal graphical display of the experimental results is provided in Figs. 3 and 4. Adjoining each of the double-reciprocal plots are the plots of the slopes and intercepts versus NADH concentration. Although the slopes and the intercepts are both functions of the concentration of NADH, when malate was the varied substrate the
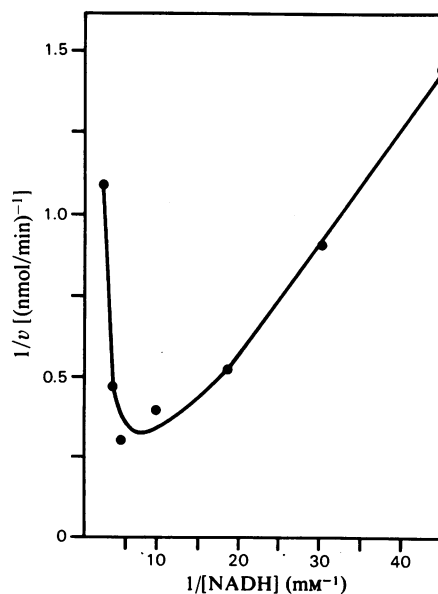

Fig. 2. *Substrate inhibition by NADH of the carboxylation reaction catalysed by NAD(P)$^+$ malic enzyme*
For full experimental details see the text. The reaction mixture (1.0 ml) contained 0.18 M-triethanolamine/HCl, 1.2 mM-MnCl$_2$, 142 mM-KHCO$_3$, 40 mM-pyruvic acid, 3 μg of protein and NADH at the indicated concentration at final pH 7.4 at 23°C.

Table 2. *Quantification of NAD$^+$ and malate production by NAD(P)$^+$ malic enzyme*
For full experimental details see the text. The specific activities of the two preparations are different owing to the relative age and storage conditions. The malate/NAD$^+$ production ratio is the nmol of malate detected divided by the nmol of NAD$^+$ produced in each incubation.

[NADH] (μM)	Protein (μg)	Sp. activity (units/mg)	NAD$^+$ production (nmol)	Malate/NAD$^+$ production ratio
Preparation 1				
75	5.6	0.066	15.4 (40 min)	0.83
75	5.6	0.071	15.9 (40 min)	0.97
75	5.6	0.065	11.0 (30 min)	1.05
75	5.6	0.061	10.5 (30 min)	1.04
75	14	0.062	25.1 (30 min)	0.97
Preparation 2				
25	8	0.018	4.63 (32 min)	1.0
75	4	0.051	6.6 (32 min)	0.97
75	8	0.054	13.4 (32 min)	0.96

Table 3. *Apparent kinetic parameters of NAD(P)$^+$ malic enzyme*

Protein (μg)	[MnCl$_2$] (mM)	Non-varied substrate	Apparent Michaelis constant	Velocity (μmol/min per mg)	Temperature (°C)
3.75	4.5	NAD$^+$ (1 mM)	$K_a^{Mal} = 5.38 \pm 0.34$ mM	$V_f = 10.2$	31
3.75	1.2	NAD$^+$ (1 mM)	$K_a^{Mal} = 4.90 \pm 0.65$ mM	$V_f = 8.5$	31
1.2	3.0	NAD$^+$ (0.3 mM)	$K_a^{Mal} = 5.66 \pm 0.45$ mM	$V_f = 12.6$	32
3.75	1.2	NAD$^+$ (1 mM)	$K_a^{Mal} = 5.71 \pm 0.42$ mM	$V_f = 4.6$	23
1.88	1.2	L-Malate (25 mM)	$K_a^{NAD^+} = 0.180 \pm 0.016$ mM	$V_f = 9.0$	31
0.72	3.0	L-Malate (30 mM)	$K_a^{NAD^+} = 0.130 \pm 0.005$ mM	$V_f = 10.5$	32
7.5	1.2	Pyruvate (40 mM); KHCO$_3$ (142 mM)	$K_a^{NADH} = 0.239 \pm 0.016$ mM	$V_f = 1.1$	23
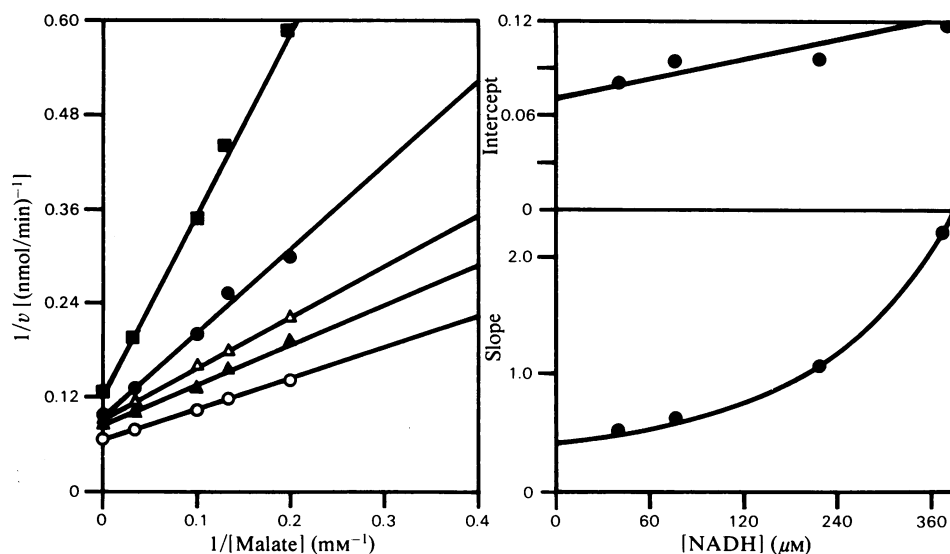
Fig. 3. *NADH product inhibition versus malate of NAD(P)$^+$ malic enzyme*
For full experimental details see the text. The reaction mixture (1.5 ml) contained 0.2 M-triethanolamine/HCl buffer, pH 7.05, 3 mM-MnCl$_2$, 300 μM-NAD$^+$, 1.2 μg of protein and NADH at concentrations (from bottom to top) 0, 20, 40, 170 and 250 μM.

Table 4. *Apparent product inhibition constants for NAD(P)$^+$ malic enzymes at 32°C*

Protein (μg)	MnCl$_2$ (mM)	Inhibitor	Non-varied substrate	Apparent inhibition constants
0.75	2.0	Pyruvate	L-Malate (25 mM)	$K_{ii} = 23.9 \pm 4.0$ mM
0.75	2.0	Pyruvate	NAD$^+$ (0.15 mM)	$K_{ii} = 15.1 \pm 2.2$ mM; $K_{is} = 11.9 \pm 0.9$ mM
1.88	1.2	NADH	L-Malate (25 mM)	$K_{ii_1} = 0.65 \pm 0.042$ mM; $K_{is_1} = 0.063 \pm 0.004$ mM $K_{ii_2} = 0.22 \pm 0.030$ mM; $K_{is_2} = 0.007 \pm 0.006$ mM
1.2	3.0	NADH	NAD$^+$ (0.3 mM)	$K_{ii} = 0.36 \pm 0.069$ mM; $K_{is_1} = 0.0088 \pm 0.010$ mM $K_{is_2} = 0.0.13 \pm 0.014$ mM

secondary plot of slope versus NADH concentration is not linear. When NAD$^+$ was the varied substrate the slopes and the intercepts of the double-reciprocal plots were both functions of NADH concentrations, but neither of the secondary plots was linear. Since the secondary plots do not result in good agreement with second-order polynomial analysis, we have assumed that these are composites of two linear functions. Table 4 includes estimates of the apparent inhibition constants for NADH based on this assumption.

Product inhibition by pyruvate

In order to ascertain the binding sequence of the substrates, the product inhibition by pyruvate was investigated. The double-reciprocal graphical dis-
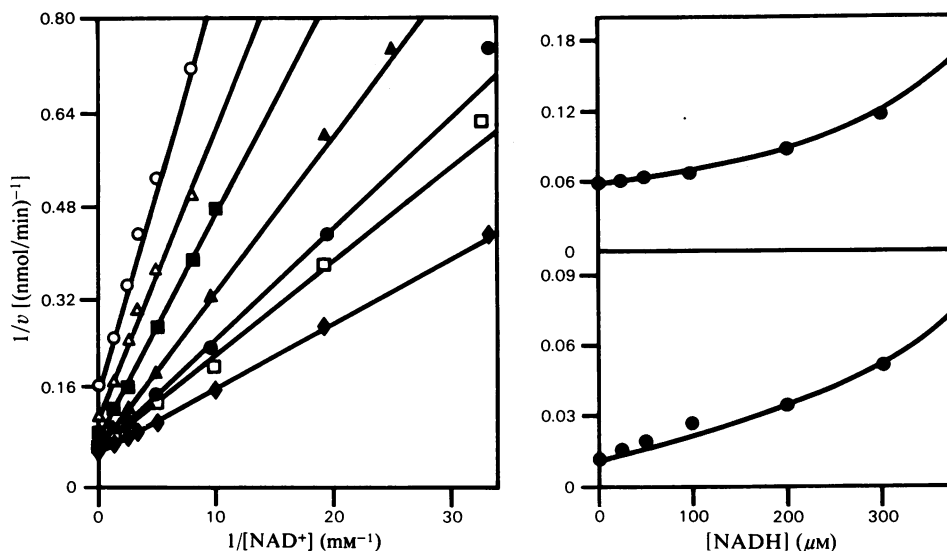
Fig. 4. *NADH product inhibition versus NAD+ of NAD(P)+ malic enzyme*

For full experimental details see the text. The reaction mixture (1.5 ml) contained 0.2 M-triethanolamine/HCl buffer, pH 7.05, 1.12 mM-MnCl$_2$, 25 mM-malate, 1.88 μg of protein and NADH at concentrations (from bottom to top) 0, 25, 50, 100, 200, 300 and 375 μM.
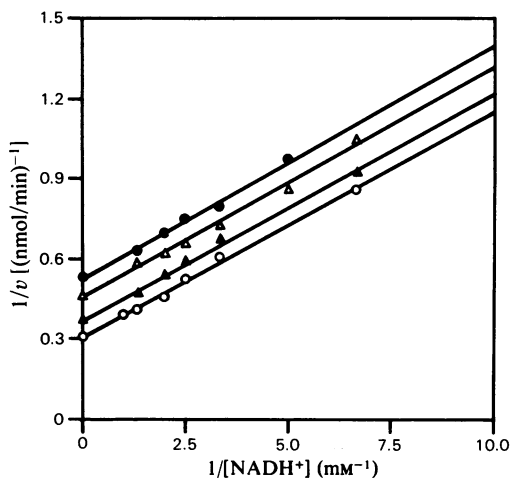

Fig. 5. *Pyruvate product inhibition versus NAD+ of NAD(P)+ malic enzyme*

For full experimental details see the text. The reaction mixture (1.5 ml) contained 0.2 M-triethanolamine/HCl buffer, pH 7.05, 2 mM-MnCl$_2$, 25 mM-malate, 0.75 μg of protein and pyruvate at concentrations (from bottom to top) 0, 4, 8 and 16 mM.
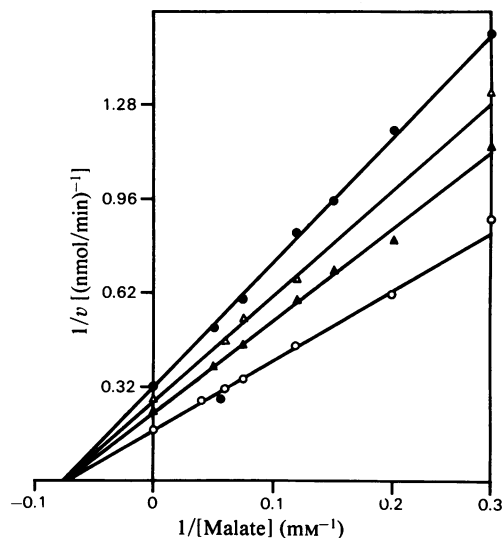

Fig. 6. *Pyruvate product inhibition versus malate of NAD(P)+ malic enzyme*

For full experimental details see the text. The reaction mixture (1.5 ml) contained 0.2 M-triethanolamine/HCl buffer, pH 7.05, 2 mM-MnCl$_2$, 150 μM-NAD+, 1.13 μg of protein and pyruvate at concentrations (from bottom to top) 0, 3.33, 6.67 and 10 mM.

play of these data is presented in Figs. 5 and 6. These data were collected with the fluorimetric assay as described in the Materials and methods section. At a saturating concentration of malate, pyruvate proved to be an anti-competitive inhibitor (Laidler & Bunting, 1973) with respect to NAD+ (Fig. 5). When NAD+ was present at a subsaturating concentration and malate was the varied substrate, pyruvate was a non-competitive inhibitor (Fig. 6). These data suggest that the steady-state kinetic mechanism involves an or-

dered binding of the substrates malate and NAD+. The binding sequence appears to be NAD+ first followed by malate. The data presented here are inadequate for the analysis of the order of pyruvate and CO_2 release.

Any plausible steady-state kinetic mechanism must account for the inhibition patterns that occur at the higher NADH concentrations. The NADH appears to bind to a form of the enzyme that is kinetically distinct from that which binds NAD+.
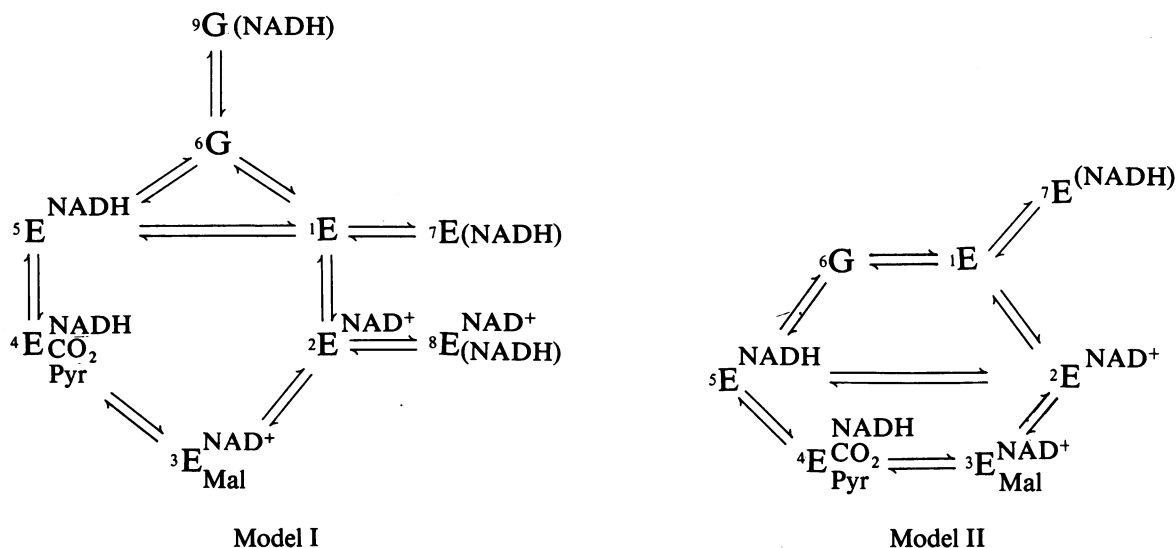
Model I   Model II

Scheme 1

The reformulated rate equation for Model I is as follows:

$$\frac{1}{v_{\text{NAD}^+}} = \frac{K_a}{V_f}\left[\frac{1+\dfrac{[\text{NADH}]}{K_{ir_3}}+\dfrac{[\text{NADH}]^2}{K_{ir_3}K_{ir_4}}}{1+\dfrac{[\text{NADH}]}{K_{ir_5}}}+\frac{K_{ib}}{[\text{Mal}]}\left(\frac{\dfrac{K_{ia}K_b}{K_aK_{ib}}+\dfrac{[\text{NADH}]}{K_{ir_3}}+\dfrac{[\text{NADH}]^2}{K_{ir_3}K_{ir_1}}}{1+\dfrac{[\text{NADH}]}{K_{ir_1}}}\right)\right]\frac{1}{[\text{NAD}^+]}$$

$$+\frac{1}{V_f}\left[\frac{1+\dfrac{[\text{NADH}]}{K_{ir_5}}}{1+\dfrac{[\text{NADH}]}{K_{ir_1}}}+\frac{K_b}{[\text{Mal}]}\left(\frac{1+\dfrac{[\text{NADH}]}{K_{ir_2}}+\dfrac{[\text{NADH}]^2}{K_{ir_2}K_{ir_6}}}{1+\dfrac{[\text{NADH}]}{K_{ir_1}}}\right)\right]$$

$$\frac{1}{v_{\text{Mal}}} = \frac{K_b}{V_f}\left[\frac{1+\dfrac{[\text{NADH}]}{K_{ir_2}}+\dfrac{[\text{NADH}]^2}{K_{ir_2}K_{ir_6}}}{1+\dfrac{[\text{NADH}]}{K_{ir_1}}}+\frac{K_aK_{ib}}{K_b[\text{NAD}^+]}\left(\frac{\dfrac{K_{ia}K_b}{K_aK_{ib}}+\dfrac{[\text{NADH}]}{K_{ir_3}}+\dfrac{[\text{NADH}]^2}{K_{ir_3}K_{ir_4}}}{1+\dfrac{[\text{NADH}]}{K_{ir_1}}}\right)\right]\frac{1}{[\text{Mal}]}$$

$$+\frac{1}{V_f}\left[\frac{1+\dfrac{[\text{NADH}]}{K_{ir_5}}}{1+\dfrac{[\text{NADH}]}{K_{ir_1}}}+\frac{K_a}{[\text{NAD}^+]}\left(\frac{1+\dfrac{[\text{NADH}]}{K_{ir_3}}+\dfrac{[\text{NADH}]^2}{K_{ir_3}K_{ir_1}}}{1+\dfrac{[\text{NADH}]}{K_{ir_1}}}\right)\right]$$

The intercept inhibition constants for NADH with regard to these two forms of the enzyme are significantly different (Table 4). In the same manner, this second form of the enzyme appears to be kinetically similar to that which binds L-malate.

Despite the complexity of the kinetic data, the mechanistic interpretations provided above can be incorporated into a consistent steady-state kinetic model (Scheme 1). Model I in Scheme 1 appears to be the more plausible. This model is provided with the appropriate reformulated rate equation.

References

Canellas, P. F. & Wedding, R. T. (1980) *Arch. Biochem. Biophys.* **199**, 259–264

Canellas, P. F., Grissom, C. B. & Wedding, R. T. (1983) *Arch. Biochem. Biophys.* **220**, 116–133

Cleland, W. W. (1979) *Methods Enzymol.* **63**, 103–138

Fisher, D. D. & Schulz, A. R. (1969) *Math. Biosci.* **4**, 189–200

Fodge, D. W., Gracy, R. W. & Harris, B. G. (1972) *Biochim. Biophys. Acta* **268**, 271–284

Frenkel, R. (1975) *Curr. Top. Cell. Regul.* **9**, 157–181

Grissom, C. B., Canellas, P. F. & Wedding, R. T. (1983) *Arch. Biochem. Biophys* **220**, 133–144

Grover, S. D., Canellas, P. F. & Wedding, R. T. (1981) *Arch. Biochem. Biophys.* **209**, 396–407

Hansford, R. G. & Lehninger, A. L. (1973) *Biochem. Biophys. Res. Commun.* **51**, 480–486

Hsu, R. Y., Lardy, H. A. & Cleland, W. W. (1967) *J. Biol. Chem.* **242**, 5315–5322

Laidler, K. J. & Bunting, P. S. (1973) *The Chemical Kinetics of Enzyme Action*, 2nd edn., p. 91, Clarendon Press, Oxford

Landsperger, W. J., Fodge, D. W. & Harris, B. N. G. (1978) *J. Biol. Chem.* **253**, 1868–1873

Lin, R. C. & Davis, E. J. (1974) *J. Biol. Chem.* **249**, 3867–3875

Lowry, O. H. & Passonneau, J. V. (1972) *A Flexible System of Enzymatic Analysis*, pp. 201–204, Academic Press, New York

Macrae, A. R. (1971) *Biochem. J.* **122**, 495–501

Mandella, R. D. & Sauer, L. A. (1975) *J. Biol. Chem.* **250**, 5877–5884

Mollering, H. (1974) in *Methods of Enzymatic Analysis* (Bergmeyer, H. U., ed.), 2nd edn., vol. 3, pp. 1589–1592, Academic Press, New York

Nagel, W. O., & Sauer, L. A. (1982) *J. Biol. Chem.* **257**, 12405–12411

Sauer, L. A. (1973*a*) *Biochem. Biophys. Res. Commun.* **50**, 524–531

Sauer, L. A. (1973*b*) *FEBS Lett.* **33**, 251–255

Walter, C. H. & Barrett, M. J. (1969) *Enzymologia* **38**, 147–160

Webb, J. L. (1966) *Enzyme and Metabolic Inhibitors*, vol. 2, pp. 432–428, Academic Press, New York

Wilkinson, G. N. (1961) *Biochem. J.* **80**, 324–336